

Chondrocranial, hyobranchial and internal oral morphology in larvae of the basal bufonid genus *Melanophryniscus* (Amphibia: Anura)

Peter M. Larson,¹ Rafael O. de Sá² and Diego Arrieta³

¹Department of Biological Sciences, Ohio University, Athens, Ohio 45701, USA;

²Department of Biology, University of Richmond, Virginia 23173, USA; and

³Carlos Casaravilla 866, C.P. 12900, Montevideo, Uruguay

Keywords:

Bufonidae, chondrocranium, internal oral morphology, *Melanophryniscus*

Accepted for publication:

16 January 2003

Abstract

Larson, P. M., de Sá, R. O. and Arrieta, D. 2003. Chondrocranial, hyobranchial and internal oral morphology in larvae of the basal bufonid genus *Melanophryniscus* (Amphibia: Anura). — *Acta Zoologica* (Stockholm) 84: 145–154

Melanophryniscus is a genus of small toads inhabiting the southern portion of South America. This genus is considered basal within the family Bufonidae. Data on larval chondrocranial morphology do not exist for the genus and larval internal oral anatomy has only been described for a single species. Here, we describe chondrocranial and internal oral morphology in *Melanophryniscus montevidensis*, *M. orejasmirandai* and *M. sanmartini*. Chondrocranial morphology is similar among the species examined. Comparisons with other bufonids and with outgroup taxa suggest that the following chondrocranial characters may represent synapomorphies for the Bufonidae: free (or absent) ceratobranchial IV, a reduced or absent larval crista parotica, the lack of a larval otic process, and late development of thin, poorly chondrified orbital cartilages. The presence of an elongated processus anterior dorsalis of the suprarostral alae and the absence of a chondrified commissura quadratoorbitalis appear to be unique in *Melanophryniscus* among bufonids. Internal oral anatomy is conserved in *Melanophryniscus*, and among bufonids in general.

Peter M. Larson, Department of Biological Sciences, Ohio University, Athens, Ohio 45701, USA. E-mail: peter.larson@ohiou.edu

Introduction

Members of the genus *Melanophryniscus* (Anura: Bufonidae) are small toads that inhabit arid and rocky areas throughout the southern portion of South America. Their range extends from the coastal lowlands of southern Brazil, through Paraguay and Uruguay, and south to northern Argentina (Frost 2002). The genus is comprised of approximately 14 species aggregated into four species-groups: the *stelzneri* group, the *rubriventris* group, the *moreirae* group, and the *tumifrons* group (Lavilla and Vaira 1997; Frost 2002). Phylogenetic relationships among species are not well defined (Langone 1994). Despite the lack of information on intrageneric relationships, the monophyly of the genus is supported by several characters (Graybeal and Cannatella 1995), and a recent phylogenetic hypothesis for the Bufonidae suggests that

Melanophryniscus is a basal member of the family (Graybeal 1997).

Characters from larval internal morphology have been increasingly used in studies of evolutionary relationships among anurans (Sokol 1975, 1981; Wassersug 1980; Wassersug and Heyer 1988; Haas 1996, 1997; Maglia *et al.* 2001). However, only a few studies have addressed variation in chondrocranial characters among closely related taxa (e.g. Haas 1995, 1996; Larson and de Sá 1998); this partially stems from a lack of baseline comparative data among closely related species. Similarly, although data on internal oral morphology are available for a variety of anuran families, the overall number of species for which descriptions are available remains relatively low (Wassersug 1980; Viertel 1982; Wassersug and Duellman 1984; Wassersug and Heyer 1988).

Chondrocranial morphology has not been reported for *Melanophryniscus* and data on internal oral morphology are only available for *Melanophryniscus stelzneri* (Echeverría 1998a). Thus, the goals of the present study are to describe and compare chondrocranial and internal oral morphology among three species of *Melanophryniscus*: *M. montevidensis*, *M. sanmartini* and *M. orejasmirandai*. These species represent the *stelzneri*, *moreirae* and *tumifrons* species-groups, respectively (Frost 2002). The morphological data presented here are compared to information available for other bufonids and outgroup taxa to provide insight into the distribution of character states in the Bufonidae.

Materials and Methods

Specimens of *Melanophryniscus orejasmirandai* (Prigioni and Langone 1986) and *M. sanmartini* (Klappenbach 1968) were collected from Sierra de Animas, Maldonado, Uruguay. Specimens of *M. montevidensis* (Philippi 1902) were collected from La Paloma, Rocha, Uruguay. All specimens were preserved in 4% formalin. A total of nine tadpoles of *M. orejasmirandai*, five tadpoles of *M. sanmartini* and nine tadpoles of *M. montevidensis* were staged (Gosner 1960), cleared, and double-stained for bone and cartilage for analysis of their chondrocranial anatomy (Dingerkus and Uhler 1977). Specimens are deposited in the United States National Museum of Natural History, Smithsonian Institution (USNM 556001–556023). Illustrations were made using a Wild MC3 Stereomicroscope with a camera lucida attachment. Chondrocranial terminology follows de Sá (1988) and Haas (1995, 1997). Chondrocrania of all three species are described as one; species divergences from the basic description are noted where necessary. As a result of the lack of a complete ontogenetic series for these species, developmental timing data reflect the earliest available stage at which a particular structure could be identified.

For scanning electron microscopy, specimens were dissected (two *M. orejasmirandai*, stage 36; *M. montevidensis*, stage 36; *M. sanmartini*, stage 37) and initially fixed in 4% formalin. Specimens were subjected to an ultrasonic wash for 15 min, fixed in a 3–4% glutaraldehyde solution for 3–4 h at room temperature, put through three 15-min washes in 0.1 M phosphate buffer, followed by secondary fixation for 2 h in a 1% solution of osmium tetroxide, after which three additional 15-min washes in 0.1 M phosphate buffer were performed. Next, all specimens were dehydrated through the use of 15-min changes in a graded ethanol series as follows: 35%, 50%, 70%, 80%, 95%, and three changes of 100%. Specimens were critical point dried in CO₂, mounted on aluminium discs and sputter coated with gold/palladium, 30 nm thick, using a Hummer VII sputtering system. Features of dorsal and ventral internal oral anatomy were examined using a Hitachi S-2300 scanning electron microscope at 15 kV and were photographed using Polaroid 55 positive/negative film. Terminology used to describe features of the

oral cavity follows Wassersug (1976, 1980) and Wassersug and Heyer (1988).

Results

Chondrocranial morphology

The overall width of the chondrocranium in *Melanophryniscus* is approximately 85–95% of its total length (Figs 1 and 2). The chondrocranium in *Melanophryniscus* is low in lateral view; its maximum height (at the level of the cornua trabeculae) is approximately 35% of its total length.

The suprarostrals consist of two distinct elements, the central corpus (sc) and the lateral ala (sa; Figs 1C and 2C,G). These elements are ventrally separate, but fused dorsally through a narrow strip of cartilage just ventral to their point of articulation with the cornua trabeculae. The corpora are thin cartilages that slope ventromedially from their point of attachment to the alae. They are ventromedially fused with one another, forming an overall V-shape in anterior view. The alae are large, ventrally rounded sheets of cartilage that flex posteriorly from their point of attachment to the corpora. They bear a well-developed, triangular to finger-like, processus posterior dorsalis (ppd) and an elongated processus anterior dorsalis (pad; Fig. 1A,C).

The cornua trabeculae (ct; Figs 1A and 2A,E) are long, narrow cartilages that extend anteriorly from their point of divergence from the ethmoid plate. The cornua are of virtually uniform width throughout their length and their divergence forms a sharp V-shape in dorsal view. In lateral view (Figs 1C and 2C,G), they represent about one-third of the total length of the chondrocranium and their anterior half curves ventrally to contact with the suprarostrals. A rounded processus lateralis trabeculae, which serves as the attachment site for the ligamentum quadratoethmoidale, is visible on the lateroventral margin of each of the cornua.

Posteriorly, the cornua trabeculae are confluent with the planum trabeculare anticum and the planum ethmoidale. The lamina orbitonasalis (lon; e.g. Figure 1A) begins to develop around stage 34–35 as a triangular to rounded growth of the planum ethmoidale, just dorsal to the attachment of the commissura quadratoethmoidalis anterior (cqa) to the braincase. In the most advanced developmental stages available of *M. montevidensis* (stage 38), *M. orejasmirandai* (stage 38), and *M. sanmartini* (stage 37), the tectum nasi has developed into a crescent-shaped cartilage that will eventually form the dorsal roof of the nasal capsules. In the latter two species, the septum nasi (sn) develops at approximately the same time as the tectum nasi as a rounded to finger-like process in the region just posterior to the confluence of the cornua trabeculae. This structure was not clearly identifiable in available specimens of *M. montevidensis*.

In early stages, the cranial floor in *Melanophryniscus* bears an extensive, bell-shaped fenestra basicranialis (fb). This fenestra is limited anteriorly by the planum trabecularum

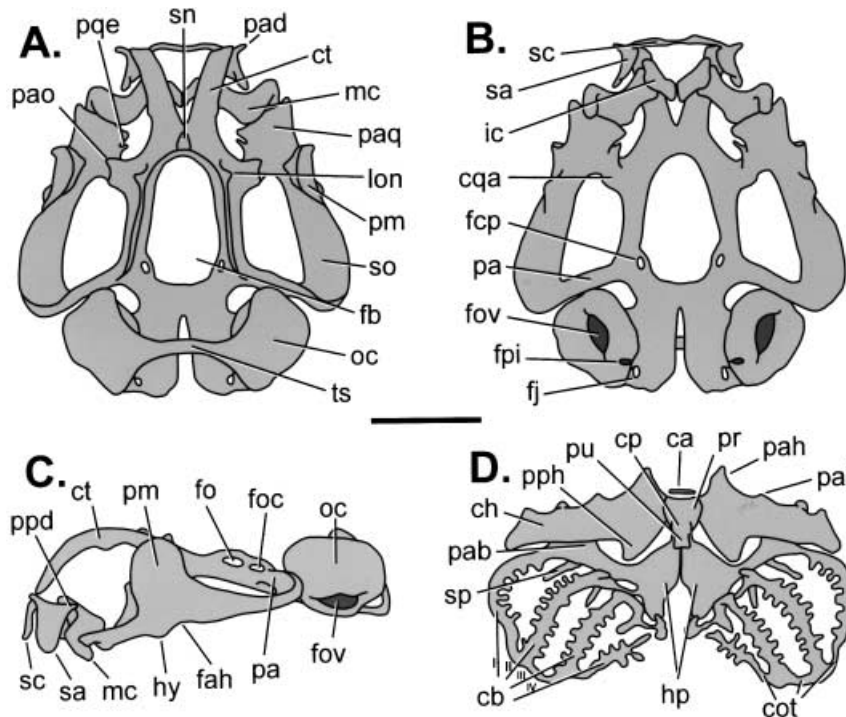


Fig. 1—Chondrocranium and hyobranchial apparatus of *Melanophryniscus orejasmirandai* (Stage 34). —**A.** dorsal, —**B.** ventral, and —**C.** lateral views of chondrocranium. —**D.** Ventral view of hyobranchial apparatus. Scale bar: 1 mm ca, copula anterior; cb I–IV, ceratobranchial cartilages I–IV; ch, ceratohyal; cot, commissurae terminales; cp, copula posterior; cqa, commissura quadrato cranialis anterior; ct, cornua trabeculae; fah, facies articularis hyalis; fb, fenestra basicranialis; fcp, foramen caroticum primarium; fj, foramen jugulare; fo, foramen opticum; foc, foramen oculomotorium; fov, fenestra ovalis; fpi, foramen perilymphaticum inferior; hp, hypobranchial plate; hy, hyoquadrate process;

ic, infrastroral cartilage; lon, lamina orbitonasalis; mc, Meckel's cartilage; oc, otic capsule; pa, processus ascendens; pab, processus anterior branchialis; pad, processus anterior dorsalis; pah, processus anterior hyalis; pal, processus anterolateralis hyalis; pao, processus antorbitalis; paq, pars articularis quadrati; pm, processus muscularis; ppd, processus posterior dorsalis; pph, processus posterior hyalis; pqe, processus quadratoethmoidalis; pr, pars reuniens; pu, processus urobranchialis; sa, suprarostrol alar; sc, suprarostrol corpus; sn, septum nasi; sp, spiculae; so, subocular bar of palatoquadrate; ts, tectum synoticum.

anticum, laterally by the thick trabeculae cranii, and posteriorly by the planum basale. Occlusion of the fenestra basicranialis has begun by stage 37 in *M. sanmartini* and is extensive by stage 38 in *M. montevidensis* and stage 36 in *M. orejasmirandai*. The planum intertrabeculare appears as a very thin, lightly chondrified sheet. In the early stages, no foramina are distinguishable in the cranial floor because of the large fenestra basicranialis. In later stages, the foramina carotica primaria (fcp) become visibly surrounded by cartilage in the posterior portion of the cranial floor. These foramina first appear as a slight indentation in the posterolateral margin of the fenestra basicranialis in a stage 35 specimen of *M. sanmartini* (e.g. Fig. 2A,B); they are fully surrounded by cartilage by stage 37. These foramina are visible earlier in the other two species, appearing completely or almost completely surrounded by cartilage (e.g. Fig. 1A,B) by stage 34. The foramina cranio-palatina were not clearly identifiable in available specimens of any species, presumably because of light chondrification of the planum intertrabeculare (Figs 1 and 2).

The lateral walls of the braincase are formed by the orbital cartilages, which extend dorsally from the posterior portions of the trabeculae cranii and anterior ends of the parachordal cartilages. Early in development, the orbital cartilages in *Melanophryniscus* are extremely low (Figs 1C and 2C,G). Later, by stage 37 in *M. sanmartini* and stage 36 in *M. orejasmirandai*, the orbital cartilages reach approximately the level of the dorsal margin of the otic capsule. When fully developed, the orbital cartilages are thin and poorly chondrified. Growth of the orbital cartilages past the level of the mid-point of the otic capsule (oc) was not observed as late as stage 38 in *M. montevidensis*. Two foramina are visible in the posterior region of the lateral walls of the braincase; the foramen opticum (fo) and the foramen oculomotorium (foc). These foramina are fully formed by stage 35 in *M. sanmartini*, stage 38 in *M. montevidensis*, and stage 34 in *M. orejasmirandai*. In earlier stages, the foramina are visible only as a ventral indentation of the dorsal margin of the trabeculae cranii (e.g. Figure 2G).

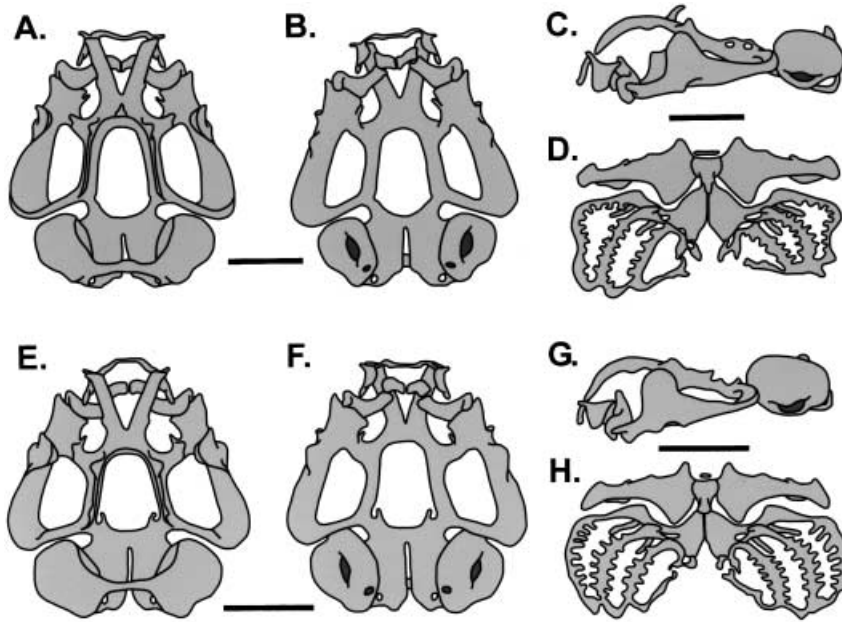


Fig. 2—Chondrocranium and hyobranchial apparatus of *Melanophryniscus sanmartini* (—A–D, Stage 35) and *M. montevidensis* (—E–H, Stage 34). —A, E, dorsal, —B, F, ventral, and —C, G, lateral views of chondrocranium. —D, H, ventral view of hyobranchial apparatus. Scale bars: 1 mm.

A large frontoparietal fenestra is visible in dorsal view. It is bordered laterally by the orbital cartilages, anteriorly by the ethmoid plate, and posteriorly by the tectum synoticum (ts). Subdivision of the frontoparietal fenestra into an anterior frontal fenestra and two posterior parietal fenestrae occurs by stage 38 in *M. orejasmirandai*. Complete subdivision of the frontoparietal fenestra was not observed in the available specimens of *M. montevidensis* and *M. sanmartini*.

The otic capsules (oc) in *Melanophryniscus* are large and ovoid. A larval crista parotica and larval otic process are absent in these species. A large fenestra ovalis (fov) is located ventrolaterally on each otic capsule (Figs 1C and 2C,G). The otic capsules are connected posteromedially via the tectum synoticum (ts), a thin cartilaginous bridge. Ventral to the point of connection of the tectum synoticum to the otic capsule, the otic capsule is confluent with the arcus occipitalis. The arcus occipitalis connects ventrally to the planum basale, thereby forming the medial and ventral margins of the foramen jugulare (fj) and the occipital condyles. The foramen perilymphaticum inferior (fpi) is present in the ventromedial region of the otic capsule, just lateral to the foramen jugulare.

The palatoquadrate is long, wide, and is orientated approximately parallel to the main body axis. The subocular bar (so) of the palatoquadrate is posterolaterally rounded; the posterior curvature of the palatoquadrate extends caudally slightly beyond the level of the anterior margin of the otic capsule (Figs 1A and 2A,E). The posterolateral margin of the palatoquadrate curls dorsally, although this is less pronounced in *M. montevidensis* (Fig. 2E). The palatoquadrate attaches to the braincase via two cartilaginous connections: the commissura quadratocranialis anterior (cqa) and the

processus ascendens (pa). The commissura quadratocranialis anterior is wide and extends ventrally and slightly anteriorly from the braincase to attach to the palatoquadrate in the region just medial to the processus muscularis quadrati (pm). It bears a well-developed, triangular processus quadratoethmoidalis (pqe) on its anterior margin. The commissura quadratocranialis anterior also bears a well-developed, rounded to finger-like processus antorbitalis (pao) projecting dorsally from its surface. A processus pseudopterygoideus is absent in these species. The processus ascendens is a narrow, rod-like bar of cartilage that extends medially and slightly anteriorly from the posteromedial margin of the palatoquadrate. It attaches to the braincase just ventral and posterior to the foramen oculomotorium (Figs 1C and 2C,G). This corresponds to a 'low' attachment condition (Sokol 1981).

The palatoquadrate also bears two anterior processes: the pars articularis quadrati (paq) and the processus muscularis quadrati (pm). The processus muscularis is wide and dorsally rounded. It extends dorsally from the lateral margin of the palatoquadrate just opposite the commissura quadratocranialis anterior. Its anterior margin curls laterally and in dorsal view it projects beyond the margin of the palatoquadrate (Figs 1A and 2A,E). The processus muscularis is inclined medially, but never contacts the processus antorbitalis. A chondrified commissura quadratoorbitalis is absent. The hyoquadrate process (hy), a rounded knob located below the processus muscularis, forms the anterior portion of the facies articularis hyalis (fah), the surface to which the ceratohyal articulates. The pars articularis quadrati, forming the anterior tip of the palatoquadrate, is wide and anteriorly expanded.

Meckel's cartilage (mc) is sigmoid in shape and articulates broadly with the pars articularis quadrati (e.g. Fig. 1A,B). This articulation is via the processus retroarticularis of Meckel's cartilage, which curls ventrally and slightly underneath the anterolateral margin of the pars articularis quadrati. Medially, Meckel's cartilage expands vertically and bears two rounded processes, the processus dorsomedialis and the processus ventromedialis. A small notch between these processes serves as the point of articulation of the infra-rostral cartilages (ic). The infra-rostral cartilages are overall rectangular, extending ventromedially from their point of articulation with Meckel's cartilages. They contact ventromedially, forming a V-shape in anterior view.

Hyobranchial morphology

The ceratohyalia (ch; Figs 1D and 2D,H) are long, wide, and are orientated perpendicular to the main body axis. They are medially flattened. Laterally, they expand in the vertical plane to articulate with the palatoquadrate at the facies articularis hyalis. Each ceratohyal bears two anterior processes; the processus anterior hyalis (pah) and the processus anterolateralis hyalis (pal). The processus anterior hyalis is located medially; it is large and triangular in shape. The processus anterolateralis hyalis is located lateral to the processus anterior hyalis and is poorly developed in all three species. Additionally, each ceratohyal bears a well-developed, triangular processus posterior hyalis (pph).

The ceratohyalia are joined medially by the pars reuniens (pr); just anterior to the pars reuniens, a small copula anterior (ca; = basihyale) is visible as a narrow sliver of cartilage. The pars reuniens attaches posteriorly to the copula posterior (cp; = basibranchial), which bears a short, stout processus urobranchialis (pu). The copula posterior is fused to the hypobranchial plates (hp). The hypobranchial plates are wide, flat, plates of cartilage that articulate medially and serve as the point of attachment of the branchial baskets. The plates are separated posteriorly by a wide, triangular to ovoid gap.

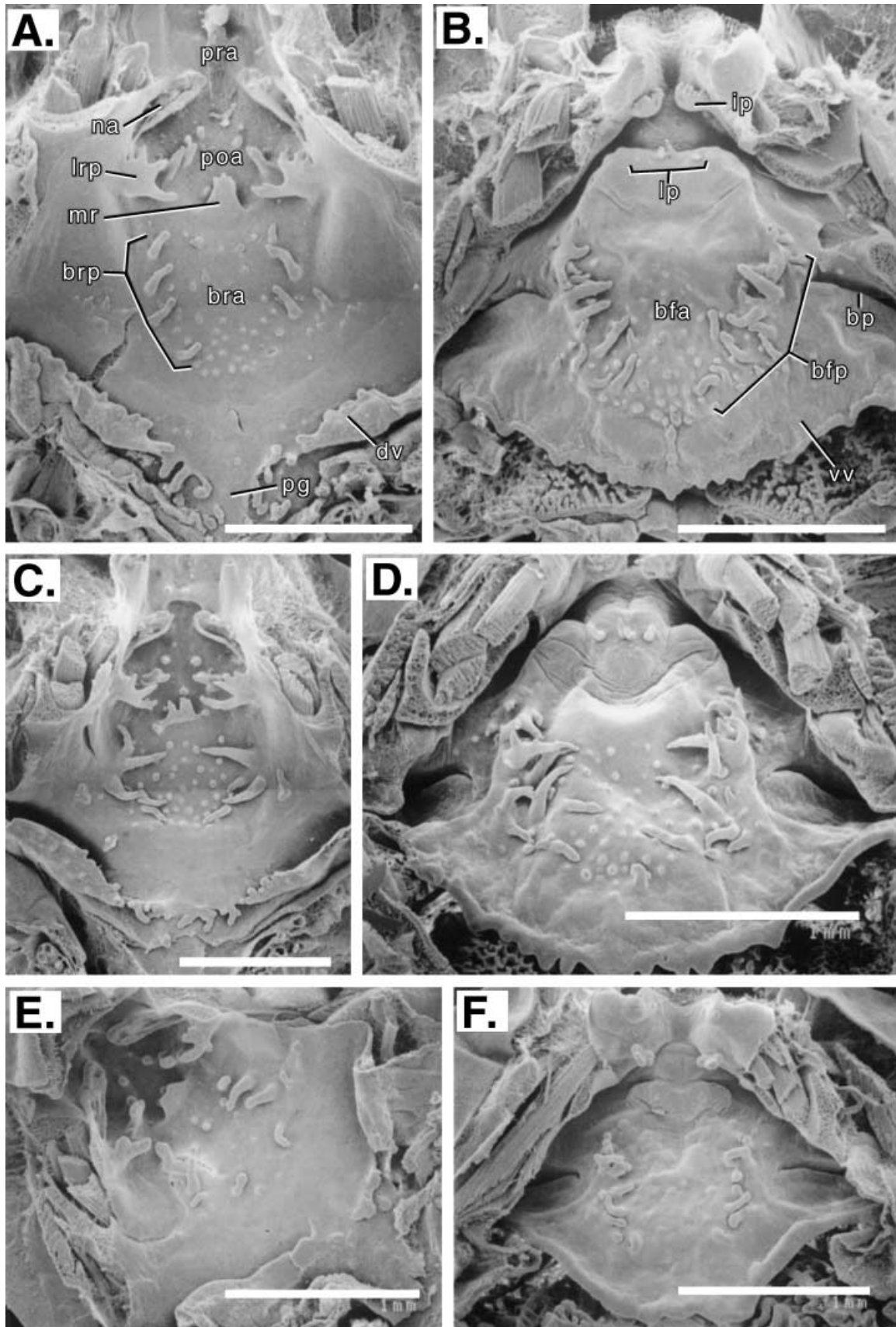
The branchial baskets consist of four ceratobranchials (cb I–IV; Figs 1D and 2D,H) that are distally connected via commissurae terminales (cot). Ceratobranchial I is continuous with the hypobranchial plate and bears a rounded processus anterior branchialis (pab) on its anterior margin. Ceratobranchial II is also continuous with the hypobranchial plate through a narrow rod of cartilage. Ceratobranchial III is connected to the hypobranchial plate by a small mass of cartilage. Proximally, ceratobranchials II and III each bear a small ventral process; the process on ceratobranchial II is large and triangular and that on ceratobranchial III is smaller and rounded. These processes do not fuse, resulting in an 'open' processus branchialis. Ceratobranchial IV is poorly developed and does not fuse to the hypobranchial plate in *Melanophryniscus* (Figs 1D and 2D,H). Although difficult to identify in many specimens, poorly stained spicules (sp.) are

present extending dorsally near the proximal ends of ceratobranchials I, II and III; these are blunt, thick, and relatively short. Also, small rod-like to rounded masses of cartilage are attached to the posterior margin of the hypobranchial plate anterior to the free end of ceratobranchial IV. They are connected to the spicule of ceratobranchial III by a lightly chondrified bridge.

Internal oral morphology

Buccal roof. The buccal roof (Fig. 3A,C,E) is triangular in shape; its maximum width is approximately equal to its length. The prenarial arena (pra) is distinguished by a crescent-shaped ledge found slightly anterior to and between the nares (na); in *M. orejasmirandai* and *M. sanmartini* (Fig. 3A,C) a pair of pustulations is located anterior to the ledge. The nares are orientated at about a 45° angle to the transverse plane; in *M. sanmartini* (Fig. 3C), narial valve projections are absent, whereas they are small and rounded in the other two species. The prenarial walls are raised and thick. In *M. orejasmirandai* and *M. sanmartini* the prenarial walls are knobby medially with a few pustulations present laterally (Fig. 3A,C), whereas in *M. montevidensis* they are relatively smooth (Fig. 3E). The postnarial arena (poa) of *M. sanmartini* is characterized by two rows of three postnarial papillae that are almost parallel to the nares (Fig. 3C). The middle pair is much larger than the other two, branching slightly and having small secondary pustulations near their base. The postnarial arena of *M. orejasmirandai* (Fig. 3A) is characterized by three large, stout postnarial papillae; only two distinct postnarial papillae were visible in *M. montevidensis*. In all three species, several pustulations are scattered about the surface of the postnarial arena. Lateral ridge papillae (lrp) extend medially from the walls of the buccal roof in the region lateral or anterolateral to the median ridge. They are large, wide and antler-like with several attenuate marginal papillae in *M. sanmartini* and *M. orejasmirandai*; they are smaller and less complex in *M. montevidensis*. The median ridge (mr) is a wide, flap-like structure that extends anteriorly over the postnarial arena. Its margin is smooth and slightly concave in *M. montevidensis* (Fig. 3E), whereas in *M. orejasmirandai* (Fig. 3A) it has several small pustulations and in *M. sanmartini* (Fig. 3C) it is divided into two sections.

The buccal roof arena (bra) is overall U-shaped, delimited by rows of three to five blunt or attenuate buccal roof papillae (brp) that are approximately parallel to each other and the main axis of the body. The rows of buccal roof papillae extend posteriorly to a point about three-quarters of the way back on the buccal roof. These papillae are largest in *M. sanmartini* (Fig. 3C). Posteriorly, the lines of buccal roof papillae begin to approach each other medially. Several small papillae and pustulations are located lateral to the buccal roof papillae and the buccal roof arena is covered by numerous pustulations in *M. orejasmirandai* and *M. sanmartini* (Fig. 3A,C); only a few pustulations are present in the buccal



roof arena of *M. montevidensis* (Fig. 3E). A distinct glandular area is found on the posterior half of the dorsal velum (dv). The lateral margins of the dorsal velum are smooth in *M. montevidensis*; they are knobby in *M. orejasmirandai* and *M. sanmartini*. Posteromedially, the dorsal velum bears numerous marginal papillae in *M. sanmartini* and *M. orejasmirandai*; only a few knobby pustulations are present in *M. montevidensis*. A distinct posteromedial gap (pg) is identifiable in *M. orejasmirandai* and *M. montevidensis* (Fig. 3A,E).

Buccal floor. The buccal floor in *Melanophryniscus* is overall triangular in shape; its length is approximately equal to its width (Fig. 3B,D,F). A large pair of infralabial papillae (ip) projects dorsomedially from the lateral margins of the most anterior portion of the buccal floor. They are elongated, anteroposteriorly compressed, and their margin has several short, attenuate secondary papillae in *M. orejasmirandai* and *M. sanmartini* (Fig. 3B,D); they are smaller with a lobed tip in *M. montevidensis* (Fig. 3F). Two pairs of transversely aligned lingual papillae (lp) project dorsally from the anteromedial region of the buccal floor; in *M. orejasmirandai* (Fig. 3B) these papillae are all attenuated and in *M. sanmartini* (Fig. 3D) the lateral pair is blunt. No lingual papillae were observed in *M. montevidensis* (Fig. 3F), although several pustulations were present in the region where these papillae are typically found.

The buccal floor arena (bfa) is large and U-shaped, narrowing slightly posteriorly. The buccal floor arena is defined by uneven rows of attenuate or blunt buccal floor papillae (bfp) that run approximately parallel to one another and extend posteriorly from a point anterior to the buccal pockets. These vary in number: more than 10 buccal floor papillae in *M. orejasmirandai* and *M. sanmartini* (Fig. 3B,D) and only seven or eight in *M. montevidensis* (Fig. 3F). The papillae are largest medial to the buccal pockets, whereas the posterior papillae are simple and smaller. These papillae are overall smaller in *M. montevidensis* (Fig. 3F). Numerous pustulations are scattered among the buccal floor papillae and on the surface of the buccal floor arena in *M. orejasmirandai* and *M. sanmartini* (Fig. 3B,D); only a few small pustulations are present on the buccal floor arena in *M. montevidensis* (Fig. 3F). In *M. orejasmirandai* (Fig. 3B), a medial row of large pustulations runs from the most posterior part of the buccal floor arena almost to the edge of the ventral velum. The buccal pockets (bp) are transversely orientated, angling slightly posteriorly on their lateral half; several pustulations are located anterior to the buccal pockets in *M. orejasmirandai* and *M. sanmartini*. The free surface of the ventral velum (vv) constitutes approximately one-quarter to one-third of the

length of the buccal floor and its posterior surface is glandular; small secretory pits are visible on the velar margin. The posterior margin of the ventral velum in *M. sanmartini* (Fig. 3D) appears smooth laterally and it has four or five knobby marginal projections on each side medially; in *M. montevidensis* (Fig. 3F) it is smooth and undulating, with no marginal projections. In *M. orejasmirandai* (Fig. 3B) the ventral velum has three triangular marginal projections on each side that appear to overlie branchial baskets I, II and III; it also bears two or three small, rounded marginal projections medially. No distinct median notch is present in these species.

Discussion

Chondrocranial morphology is similar among the examined species of *Melanophryniscus* (Figs 1 and 2). They are characterized by: (i) quadripartite suprarostal cartilages with both anterior and posterior dorsal processes, ventrally separate and dorsally confluent pars corporis and pars alaris; (ii) narrow, long and widely divergent cornua trabeculae; (iii) late development of thin, poorly chondrified orbital cartilages; (iv) larval otic process and crista parotica absent; (v) commissura quadratoorbitalis absent; (vi) low attachment of the processus ascendens; (vii) processus lateralis trabeculae present; (viii) processus quadratoethmoidalis present; (ix) processus pseudopterygoideus absent; (x) pars articularis long and anteriorly expanded; (xi) subocular bar of palatoquadrate laterally rounded, extending just past the anterior margin of the otic capsule; (xii) copula anterior (= basihyale) present; (xiii) ceratohyal with processus anterior hyalis, processus anterolateralis hyalis, and processus posterior hyalis; (xiv) ceratobranchial IV poorly developed and free from the hypobranchial plate; and (xv) 'open' processus branchialis.

Recent research indicates that variation in chondrocranial morphology in larval anurans can be phylogenetically informative, even among closely related taxa (Haas 1995, 1996; Larson and de Sá 1998; Maglia *et al.* 2001). Thus, we discuss variation in chondrocranial morphology among bufonids in the context of a recent phylogenetic hypothesis for the Bufonidae (Graybeal 1997). In addition to data presented here on *Melanophryniscus*, chondrocranial data are available for the following other bufonids: *Atelopus tricolor* and *Atelophryniscus chrysophorus* (Lavilla and de Sá 2001), *Bufo americanus* (Parker 1881; Wassersug and Hoff 1982; personal observation), *B. angusticeps* (Barry 1956), *B. arenarum* (Fabrezi and Vera 1997), *B. bufo* (Parker 1876; Ridewood 1898; Haas 1995, 1996), *B. melanostictus* (Ramaswami 1940), *B.*

Fig. 3—Scanning electron micrographs of —**A, C, E**, the buccal roof and —**B, D, F**, the buccal floor in *Melanophryniscus orejasmirandai* (—**A, B**, Stage 36), *M. sanmartini* (—**C, D**, Stage 37) and *M. montevidensis* (—**E, F**, Stage 36). Scale bars: 1 mm bfa, buccal floor arena; bfp, buccal floor papillae; bp, buccal pocket;

bra, buccal roof arena; brp, buccal roof papillae; dv, dorsal velum; ip, infralabial papillae; lp, lingual papillae; lrp, lateral ridge papillae; mr, median ridge; na, nares; pg, posteromedial gap; poa, postnarial arena; pra, prenarial arena; vv, ventral velum.

paracnemis (Fabrezi and Vera 1997), and *B. regularis* (Sedra 1950; Sedra and Michael 1958). These studies vary in the amount of information provided by descriptions and illustrations, often as a result of a focus on a particular subset of chondrocranial structures. As a result, character states could not always be determined for all of the above species.

Since relationships within the Neobatrachia remain unresolved (Ford and Cannatella 1993; Hedges and Maxson 1993; Hillis *et al.* 1993), identifying appropriate outgroups for the examination of phylogenetic patterns within the Bufonidae remains difficult. Given this uncertainty, we follow Graybeal (1997) in choice of outgroup genera and use chondrocranial data from the following outgroup taxa: *Leptodactylus pentadactylus* (Larson and de Sá 1998), *Rana catesbeiana* (Gradwell 1972; personal observation), and *Hyla cinerea* (Haas 1996). We omit two additional outgroup taxa from the study by Graybeal (1997), *Xenopus laevis* and *Ceratophrys ornata*, because of their highly specialized larvae (Lavilla and Fabrezi 1992; Trueb and Hanken 1992; Wild 1997).

Comparisons of available data for bufonids with outgroup species indicate that several characters may represent synapomorphies for the Bufonidae. These include (outgroup states in parentheses): (i) The absence of a larval otic process and (ii) a reduced or absent larval crista parotica are both shared by *Melanophryniscus* (present study), *Bufo americanus* (Parker 1881; personal observation), *B. angusticeps* (Barry 1956), *B. arenarum* (Fabrezi and Vera 1997), *B. bufo* (Haas 1995), *B. paracnemis* (Fabrezi and Vera 1997), *B. regularis* (Sedra 1950), *Atelopus tricolor* and *Atelophryniscus chrysophorus* (Lavilla and de Sá 2001) (larval otic process present in *Rana* and *Hyla*, absent in *Leptodactylus*; well developed larval crista parotica present in all outgroups); (iii) a poorly developed ceratobranchial IV, not fused to the hypobranchial plate, is shared by *Melanophryniscus* (present study), *B. americanus* (personal observation), *B. paracnemis* (Fabrezi and Vera 1997), and *B. regularis* (Sedra 1950; ceratobranchial IV connected to the hypobranchial plate in outgroups). Ceratobranchial IV is also reduced or vestigial in *Atelopus tricolor* and *Atelophryniscus chrysophorus* (Lavilla and de Sá 2001; Haas, personal communication).

A fourth potential bufonid synapomorphy involves the development of the orbital cartilages. The following bufonid species have been illustrated or described as having low or poorly developed orbital cartilages: *Atelopus tricolor*, *Atelophryniscus chrysophorus* (Lavilla and de Sá 2001), *Bufo angusticeps* (Barry 1956), and *B. melanostictus* (Ramaswami 1940). In contrast, other studies illustrate *B. americanus* and *B. regularis* as having fully developed orbital cartilages (Sedra 1950; Wassersug and Hoff 1982). In outgroup taxa, orbital cartilages are developed prior to stage 30 in *Leptodactylus* and *Rana*, although the latter never appears to fully chondrify the medial portion of the orbital cartilage. Available data do not permit determination of the exact timing of formation of the orbital cartilages in *Hyla cinerea* (Haas 1996), however, com-

plete or nearly complete formation of these cartilages by stage 30 has been observed in several other hylids (e.g. *Litoria genimaculata*, Haas and Richards 1998; *Hyla geographica*, d'Heursel and de Sá 1999; *Agalychnis callidryas*, personal observation).

In *Melanophryniscus*, the orbital cartilages are low in early stage specimens (< stage 36–37). In later stage specimens, dorsal extension of the orbital cartilages consists of an extremely thin, poorly chondrified sheet of cartilage that reaches approximately to the level of the dorsal margin of the otic capsule when fully developed. Our examination of a series of *B. americanus* ($n > 100$) larvae indicates that in late-stage specimens of this species (> stage 36), the orbital cartilages are also fully developed and appear as a thin cartilaginous sheet extending dorsally from the thick trabeculae cranii. The orbital cartilages stain poorly with alcian blue in whole-mount specimens of both *Melanophryniscus* and *Bufo americanus*, and thus are typically only visible in very well-stained specimens. Although we lack detailed developmental data for most bufonid taxa, we would suggest that this pattern of low, poorly developed orbital cartilages early in ontogeny, and late ontogenetic development of a thin, poorly chondrified dorsal orbital cartilage may represent a synapomorphy for the Bufonidae.

Characters that seem to be unique to *Melanophryniscus* among bufonids are also identifiable. A chondrified commissura quadratoorbitalis is present in *Atelophryniscus chrysophorus* and *Atelopus tricolor* (Lavilla and de Sá 2001), *Bufo americanus* (personal observation), *Bufo angusticeps* (Barry 1956), *B. arenarum* (Fabrezi and Vera 1997), *B. bufo* (Haas 1995), *B. melanostictus* (Ramaswami 1940), *B. paracnemis* (Fabrezi and Vera 1997), *B. regularis* (Sedra 1950), and *B. terrestris* (Sokol 1981). A chondrified commissura quadratoorbitalis is lacking in the species of *Melanophryniscus* examined here. Additionally, *Melanophryniscus* have an elongated, finger-like, processus anterior dorsalis extending anterolaterally from the dorsomedial margin of the supra-rostral alae, near the articulation of these cartilages with the trabecular horns. This process has not been reported for any other bufonid; to our knowledge it has only been reported in *Cycloramphus stejnegeri* (Leptodactylidae; Lavilla 1991). This structure may represent a synapomorphy for *Melanophryniscus* within the Bufonidae, although detailed analysis of other bufonids is necessary.

A few characters appear to be highly variable among bufonids and are consequently of questionable taxonomic importance. For example, the copula anterior (= basihyale) is absent in *Atelopus tricolor* (Lavilla and de Sá 2001), *B. bufo* (Haas 1995), and *B. paracnemis* (Fabrezi and Vera 1997) and its presence was not reported for *B. angusticeps* (Barry 1956). Conversely, a copula anterior is present in *B. arenarum* (Fabrezi and Vera 1997), *B. regularis* (Sedra and Michael 1958), and *Atelophryniscus chrysophorus* (Lavilla and de Sá 2001). Furthermore, its presence is intraspecifically variable in *B. americanus* (personal observation). The copula anterior is

present as a small sliver of cartilage in all three species of *Melanophryniscus* examined here. Also, a ‘ball-like swelling’ of spicule IV that remains attached to the hypobranchial plate was reported in *B. regularis* (Sedra and Michael 1958). Similar structures on the posterior margin of the hypobranchial plate, just anterior to the free end of ceratobranchial IV, were observed in *Melanophryniscus* and *B. americanus* (personal observation). These structures are absent in *A. tricolor* and *A. chrysophorus* (Lavilla & de Sá 2001). These structures may correspond to a vestigial spicule IV.

Data on internal oral anatomy in bufonids is currently limited to a few genera: *Ansonia* (Inger 1985), *Bufo* (Viertel 1982; Inger 1985; Echeverría 1998a,b), *Melanophryniscus* (Echeverría 1998a), and *Pedostibes* (Inger 1985). Available data for bufonids indicate that internal oral anatomy in the Bufonidae is conserved; broader discussions of taxonomic variation in oral morphology are provided by Wassersug (1980) and Viertel and Richter (1999). Overall, in *Melanophryniscus* (Fig. 3) the shape and relative dimensions of the buccal floor and roof are similar among species for which data are available (*M. stelzneri*, Echeverría 1998a; present study). Buccal floor characteristics shared by the four are: the presence of a single pair of infralabial papillae, a U-shaped buccal floor arena bounded by papillae, similar structure of buccal pockets, and similar arrangement of buccal floor arena papillae. Shared buccal roof characteristics include a crescent-shaped ledge in the prenarial arena, reduced (or absent) narial valve, one or more pairs of postnarial papillae, single pair of lateral ridge papillae, distinct median ridge, and a U-shaped buccal roof arena.

Internal oral anatomy in *Melanophryniscus montevidensis* presents several differences when compared to *M. sanmartini* and *M. orejasmirandai*. Most differences involve structures being smaller and/or less complex in *M. montevidensis*. Also, fewer pustulations and/or papillae are present on the buccal roof and floor in *M. montevidensis*. However, limited availability of specimens precludes us from making definitive statements regarding interspecific differences. *Melanophryniscus sanmartini*, *M. orejasmirandai* and *M. stelzneri* (Echeverría 1998a) share the following characters: (i) complex infralabial papillae with highly serrate and jagged margins; (ii) two pairs of large lingual papillae; (iii) large, conical buccal floor arena papillae; (iv) ventral velum with numerous marginal projections; (v) complex, antler-like lateral ridge papillae; and (vi) surface of buccal floor arena highly pustulate. A few differences are also noted from available data for these three species. First, a distinct posteromedial gap was identifiable in all species except *M. sanmartini*. Second, a distinct internarial projection is present in *M. stelzneri* (Echeverría 1998a); we found no such projection in the three species examined here. Third, *M. orejasmirandai* is unique among *Melanophryniscus* in having a medial line of pustulations extending from the posterior margin of the buccal floor arena onto the ventral velum.

Conclusion

Currently, *Melanophryniscus* is hypothesized as a basal genus of bufonids (Graybeal 1997). The monophyly of the Bufonidae is supported by four chondrocranial characters identified above – free (or absent) ceratobranchial IV, a reduced or absent larval crista parotica, the lack of a larval otic process, and late development of thin, poorly chondrified orbital cartilages – shared by *Melanophryniscus* and other bufonid genera. However, the lack of a larval otic process may support a larger clade because, among the outgroups considered, it is also absent in *Leptodactylus*. Although further sampling of bufonid taxa is needed, *Melanophryniscus* differs from currently described bufonids in lacking a chondrified commissura quadratoorbitalis and possessing a processus anterior dorsalis of the suprarostral. Other characters are variably present within the Bufonidae (e.g. copula anterior). Thus, data for bufonids summarized here further emphasize that variation in larval morphology is present even among closely related taxa (e.g. Larson and de Sá 1998). Such variation must be carefully considered when using larval characters in phylogenetic reconstruction at higher taxonomic levels.

Acknowledgements

We thank Chris Swart for helping with illustrations. This work was partially funded by NSF RUI # 9815787.

References

- Barry, T. H. 1956. The ontogenesis of the sound-conducting apparatus of *Bufo angusticeps* Smith. – *Morphologisches Jahrbuch* 97: 477–544.
- Dingerkus, G. and Uhler, L. D. 1977. Enzyme clearing of alcian blue stained whole small vertebrates for demonstration of cartilage. – *Stain Technology* 52: 229–232.
- Echeverría, D. D. 1998a. Microanatomía de la cavidad bucofaringea de la larva de tres bufónidos de la Argentina, con comentarios a cerca del aparato bucal y del contenido intestinal. – *Cuadernos de Herpetología* 12: 1–11.
- Echeverría, D. D. 1998b. Microanatomía del aparato bucal y de la cavidad oral de la larva de *Bufo fernandezae* Gallardo, 1957 (Anura, Bufonidae), con comentarios acerca de la coloración in vivo y la anatomía externa. – *Alytes (Paris)* 16: 50–60.
- Fabrezi, M. and Vera, R. 1997. Caracterización morfológica de larvas de anuros del Noroeste Argentino. – *Cuadernos de Herpetología* 11: 38–50.
- Ford, L. S. and Cannatella, D. C. 1993. The major clades of frogs. – *Herpetological Monographs* 7: 94–117.
- Frost, D. R. 2002. *Amphibian Species of the World: An Online Reference*. V2–21. – Electronic database available at <http://research.amnh.org/herpetology/amphibia/index.html>.
- Gosner, K. L. 1960. A simplified table for staging anuran embryos and larvae with notes on identification. – *Herpetologica* 16: 183–190.
- Gradwell, N. 1972. Gill irrigation in *Rana catesbeiana*. Part I. On the anatomical basis. – *Canadian Journal of Zoology* 50: 481–499.
- Graybeal, A. 1997. Phylogenetic relationships of bufonid frogs and tests of alternate macroevolutionary hypotheses characterizing

- their radiation. – *Zoological Journal of the Linnean Society* 119: 297–338.
- Graybeal, A. and Cannatella, D. C. 1995. A new taxon of Bufonidae from Peru, with descriptions of two new species and a review of the phylogenetic status of supraspecific bufonid taxa. – *Herpetologica* 51: 105–131.
- Haas, A. 1995. Cranial features of dendrobatid larvae (Amphibia: Anura: Dendrobatidae). – *Journal of Morphology* 224: 241–264.
- Haas, A. 1996. Das larvale cranium von *Gastrotheca riobambae* und seine metamorphose (Amphibia, Anura, Hylidae). – *Verhandlungen Des Naturwissenschaftlichen Vereins in Hamburg* 36: 33–162.
- Haas, A. 1997. The larval hyobranchial apparatus of discoglossid frogs: its structure and bearing on the systematics of the Anura (Amphibia: Anura). – *Journal of Zoological Systematics and Evolutionary Research* 35: 179–197.
- Haas, A. and Richards, S. J. 1998. Correlations of cranial morphology, ecology, and evolution in Australian suctorial tadpoles of the genera *Litoria* and *Nyctimystes* (Amphibia: Anura: Hylidae: Pelodyadinae). – *Journal of Morphology* 238: 109–141.
- Hedges, S. B. and Maxson, L. R. 1993. A molecular perspective on lissamphibian phylogeny. – *Herpetological Monographs* 7: 27–42.
- d'Heursel, A. and de Sá, R. O. 1999. Comparing the tadpoles of *Hyla geographica* and *Hyla semilineata*. – *Journal of Herpetology* 33: 353–361.
- Hillis, D. M., Ammerman, L. K., Dixon, M. T. and de Sá, R. O. 1993. Ribosomal DNA and the phylogeny of frogs. – *Herpetological Monographs* 7: 118–131.
- Inger, R. F. 1985. Tadpoles of the forested regions of Borneo. – *Fieldiana Zoology* 26: 1–89.
- Klappenbach, M. A. 1968. Notas herpetológicas IV. El género *Melanophryniscus* (Amphibia, Salientia) en el Uruguay, con la descripción de dos nuevas especies. – *Comunicaciones Zoológicas Del Museo de Historia Natural de Montevideo* 9 (118): 1–12.
- Langone, J. A. 1994. Ranas y sapos del Uruguay (Reconocimiento y aspectos biológicos). – *Museo Damaso Antonio Larrañaga, Serie de Divulgación* 5: 1–123.
- Larson, P. M. and de Sá, R. O. 1998. Chondrocranial morphology of *Leptodactylus* larvae (Leptodactylidae: Leptodactylinae): its utility in phylogenetic reconstruction. – *Journal of Morphology* 238: 287–305.
- Lavilla, E. O. 1991. Condrocáneo y esqueleto visceral en larvas de *Cycloramphus stejnegeri* (Leptodactylidae). – *Amphibia-Reptilia* 12: 33–38.
- Lavilla, E. O. and de Sá, R. 2001. Chondrocranium and visceral skeleton of *Atelopus tricolor* and *Atelophryniscus chrysophorus* tadpoles (Anura, Bufonidae). – *Amphibia-Reptilia* 22: 167–177.
- Lavilla, E. O. and Fabrezi, M. 1992. Anatomía cranial de larvas de *Lepidobatrachus llanensis* y *Ceratophrys cranwelli* (Anura: Leptodactylidae). – *Acta Zoologica Lilloana* 42: 5–11.
- Lavilla, E. O. and Vaira, M. 1997. The larva of *Melanophryniscus rubriventris rubriventris* (Vellard, 1947) (Anura, Bufonidae). – *Alytes (Paris)* 15: 19–25.
- Maglia, A. M., Púgener, L. A. and Trueb, L. 2001. Comparative development of anurans: using phylogeny to understand ontogeny. – *American Zoologist* 41: 538–551.
- Parker, W. K. 1876. On the structure and development of the skull in the Batrachia. Part II. – *Proceedings of the Zoological Society of London* 1876: 601–669.
- Parker, W. K. 1881. On the structure and development of the skull in the Batrachia. Part III. – *Philosophical Transactions of the Royal Society of London* 172: 1–266.
- Philippi, R. A. 1902. *Imp. E.* – *Suplemento a los batraquios chilenos descritos en la historia física y política de Chile de Don Claudio Gay*. Blanchard-Chessi, Santiago, Chile.
- Prigioni, C. M. and Langone, J. A. 1986. *Melanophryniscus orejasmirandai* n. sp., un nuevo Bufonidae (Amphibia, Anura) de Uruguay con una clave par las especies del grupo *tumifrons*. – *Comunicaciones Zoológicas Del Museo de Historia Natural de Montevideo* 11 (159): 1–11.
- Ramaswami, L. S. 1940. Some aspects of the chondrocranium of the South Indian frogs. – *Journal of the Mysore University* 1: 15–41.
- Ridewood, W. G. 1898. On the larval hyobranchial skeleton of the anurous batrachians with special reference to the axial parts. – *Journal of the Linnean Society of London* 26: 474–487.
- de Sá, R. O. 1988. Chondrocranium and ossification sequence of *Hyla lanciformis*. – *Journal of Morphology* 195: 345–356.
- Sedra, S. N. 1950. The metamorphosis of the jaws and their muscles in the toad, *Bufo regularis* Reuss, correlated with changes in the animal's feeding habits. – *Proceedings of the Zoological Society of London* 120: 405–449.
- Sedra, S. N. and Michael, M. I. 1958. The metamorphosis and growth of the hyobranchial apparatus of the Egyptian toad, *Bufo regularis* Reuss. – *Journal of Morphology* 103: 1–30.
- Sokol, O. M. 1975. The phylogeny of anuran larvae: a new look. – *Copeia* 1975: 1–23.
- Sokol, O. M. 1981. The larval chondrocranium of *Pelodytes punctatus* with a review of tadpole chondrocrania. – *Journal of Morphology* 169: 161–184.
- Trueb, L. and Hanken, J. 1992. Skeletal development in *Xenopus laevis* (Anura: Pipidae). – *Journal of Morphology* 214: 1–41.
- Viertel, B. 1982. The oral cavities of central European anuran larvae (Amphibia) morphology, ontogenesis and generic diagnosis. – *Amphibia-Reptilia* 3: 327–360.
- Viertel, B. and Richter, S. 1999. Anatomy: viscera and endocrines. In Altig, R. and McDiarmid, R. W. (Eds): *Tadpoles: the Biology of Anuran Larvae*, pp. 92–148. University of Chicago Press, Chicago.
- Wassersug, R. 1976. Oral morphology of anuran larvae: Terminology and general description. – *Occasional Papers of the Museum of Natural History, University of Kansas* 48: 1–23.
- Wassersug, R. 1980. Internal oral features of larvae from eight anuran families: functional, systematic, evolutionary and ecological considerations. – *Occasional Papers of the Museum of Natural History, University of Kansas* 68: 1–146.
- Wassersug, R. J. and Duellman, W. 1984. Oral structures and their development in egg-brooding hylid frog embryos and larvae: Evolutionary and ecological implications. – *Journal of Morphology* 182: 1–38.
- Wassersug, R. J. and Heyer, W. R. 1988. A survey of internal oral features of leptodactylid larvae (Amphibia: Anura). – *Smithsonian Contributions to Zoology* 457: 1–99.
- Wassersug, R. J. and Hoff, K. 1982. Developmental changes in the orientation of the anuran jaw suspension. A preliminary exploration into the evolution of anuran metamorphosis. In Hecht, M., Wallace, B. and Prace, G. (Eds): *Evolutionary Biology*, Vol. 15, pp. 223–246. Plenum Press, New York.
- Wild, E. R. 1997. Description of the adult skeleton and developmental osteology of the hyperossified horned frog, *Ceratophrys cornuta* (Anura: Leptodactylidae). – *Journal of Morphology* 232: 169–206.